



HAL
open science

Angiopoietin-1 gene transfer improves the impaired wound healing of the genetically diabetic mice without increasing VEGF expression

Alessandra Bitto, Letteria Minutoli, Maria Rosaria Galeano, Domenica Altavilla, Francesca Polito, Tiziana Fiumara, Margherita Calò, Patrizia Lo Cascio, Lorena Zentilin, Mauro Giacca, et al.

► To cite this version:

Alessandra Bitto, Letteria Minutoli, Maria Rosaria Galeano, Domenica Altavilla, Francesca Polito, et al.. Angiopoietin-1 gene transfer improves the impaired wound healing of the genetically diabetic mice without increasing VEGF expression. *Clinical Science*, 2008, 114 (12), pp.707-718. 10.1042/CS20070250 . hal-00479391

HAL Id: hal-00479391

<https://hal.science/hal-00479391>

Submitted on 30 Apr 2010

HAL is a multi-disciplinary open access archive for the deposit and dissemination of scientific research documents, whether they are published or not. The documents may come from teaching and research institutions in France or abroad, or from public or private research centers.

L'archive ouverte pluridisciplinaire **HAL**, est destinée au dépôt et à la diffusion de documents scientifiques de niveau recherche, publiés ou non, émanant des établissements d'enseignement et de recherche français ou étrangers, des laboratoires publics ou privés.

ANGIOPOIETIN-1 GENE TRANSFER IMPROVES THE IMPAIRED WOUND HEALING OF THE GENETICALLY DIABETIC MICE WITHOUT INCREASING VEGF EXPRESSION .

Alessandra Bitto¹, Letteria Minutoli¹, Maria Rosaria Galeano², Domenica Altavilla¹, Francesca Polito¹, Tiziana Fiumara¹, Margherita Calò³, Patrizia Lo Cascio⁴, Lorena Zentilin⁵, Mauro Giacca⁵ and Francesco Squadrito^{1*}.

¹Department of Clinical and Experimental Medicine and Pharmacology, Section of Pharmacology, University of Messina, Italy

²Department of Surgical Sciences, University of Messina, Italy.

³Department of Veterinary Public Health, Section of Veterinary Pharmacology and Toxicology, University of Messina, Italy

⁴Department of Animal Biology and Marine Ecology, Faculty of Science, University of Messina, Italy

⁵Molecular Medicine Laboratory, International Centre for Genetic Engineering and Biotechnology, Trieste, Italy.

Key words: Ang-1, rAAV, diabetes, wound healing, eNOS, angiogenesis, VEGF, VEGFR-2, PECAM-1.

Running title: Angiopoietin-1 improves diabetic healing

***Corresponding author:**

Prof. F. Squadrito, Department of Clinical and Experimental Medicine and Pharmacology, Section of Pharmacology, Torre Biologica 5th floor, c/o AOU Policlinico G. Martino, Via C. Valeria Gazzi, 98125, Messina, ITALY Tel. +39 090 2213648; Fax +39 090 2213300; E-mail: Francesco.Squadrito@unime.it

Abstract

Angiopoietin-1 improves the ineffective angiogenesis and the impaired wound healing of diabetes. However the mechanism underlying this positive effect is still far from being completely understood. We investigated whether rAAV-Ang-1 gene transfer could improve wound repair in genetically diabetic mice (db^+/db^+) and the mechanism(s) by which it causes new vessel formation.

An incisional skin-wound model on diabetic and normoglycaemic mice was used. After the incision animals received in the wound edge rAAV-Lac-Z or rAAV-Ang-1. After 7 and 14 days wounds were used to confirm Ang-1 gene transfer, to assess histologically the healing process, to evaluate wound breaking strength, and to study new vessel formation by PECAM-1 (platelet/endothelial cell adhesion molecule) immunostaining. Finally we investigated VEGF-mRNA and protein content, eNOS expression and VEGFR-1 and VEGFR-2 immunostaining.

The efficiency of Ang-1 gene transfer was confirmed by its increased mRNA and protein expression. rAAV-Ang-1 significantly improved the healing process stimulating reepithelization and collagen maturation, increased breaking strength and significantly augmented the number of new vessels, as indicated by PECAM-1 immunostaining. However Ang-1 gene transfer did not modify the deficient VEGF-mRNA and protein expression in diabetic mice; in contrast it increased eNOS expression, augmented nitrate wound content and VEGFR-2 immunostaining and protein expression. Ang-1 gene transfer did not change vascular permeability. Similar results were obtained in normoglycaemic animals.

Our data provide strong evidence that Ang-1 gene transfer improves the delayed wound repair in diabetes by inducing angiogenesis in a VEGF-independent manner.

INTRODUCTION

Angiogenesis is a multistep process that involves endothelial cell (EC) sprouting from the parent vessel, followed by migration, proliferation, alignment, tube formation, and anastomosis to other vessels [1]. Only under certain physiological and pathological situations, active angiogenesis occurs in the adult life. This process is associated with expression of cytokines, as well as angiogenic factors, such as VEGF [2]. Members of the VEGF family, including VEGF (also known as VEGF-A), VEGF-B, and placental growth factor, play important roles in angiogenesis. The effects of VEGF are mediated via receptors termed Flt-1 or VEGF-R1 and KDR/Flk-1 or VEGFR-2 [3]. VEGF levels are increased during hypoxic conditions, making VEGF-driven angiogenesis a central response to low oxygen tension.

Insufficient angiogenesis is involved in the impaired healing of diabetic skin ulcers [4, 5]. Indeed, healing impairment in diabetics is characterized by delayed cellular infiltration and granulation tissue formation, decreased collagen organization and, of course, reduced angiogenesis [4, 5]. As far as angiogenesis is concerned a defect in VEGF regulation, characterized by an altered expression pattern of VEGF mRNA during skin repair has been shown in db/db mice [6]. In addition to confirm the pivotal role of VEGF in skin repair abnormalities of diabetic animals, it has been reported that adeno-associated viral vector (AAV) mediated human VEGF165 gene transfer, stimulates angiogenesis and wound healing in the genetically diabetic mice [7].

Besides angiogenesis, vasculogenesis may also play a crucial role in the healing process. Vasculogenesis, the *in situ* differentiation of the primitive endothelial progenitors known as angioblasts into endothelial cells that aggregate into a primary capillary plexus, has been shown to be responsible for the development of the vascular system during embryogenesis [8]. However, vasculogenesis is also present in adults and occurs through the action of circulating or resident bone marrow-derived cells called endothelial progenitor cells (EPCs) [9]. Further cell-lineages not bone-marrow derived may be found at different sites and have been demonstrated to differentiate into endothelial cells under hypoxic conditions or during physiologic replenishment of skin and gut [10]. Moreover vasculogenesis appears more present and effective when angiogenesis is failing: this is the case of the healing of diabetic ulcers in which there is

an impairment of haemostasis, inflammation, matrix deposition and most of all angiogenesis [11].

Angiopoietins are known to work in concert with VEGF in vascular growth, development and maintenance as well as in the regulation of microvascular permeability [12]. Angiopoietin-1 has been also proposed to stimulate angiogenesis via the activation of Akt signalling pathway and finally stimulates endothelial Nitric Oxide Synthase (eNOS) [13]. This mechanism could be extremely important in the repair of wounds especially during impaired wound healing which may be a consequence of metabolic derangement such as diabetes [14].

Recently Cho and colleagues [15] reported the beneficial effects of a soluble form of Ang-1, cartilage oligomeric matrix protein (COMP)-Ang1, on promotion of healing in cutaneous wounds of diabetic mice by using an adenovirus encoding for COMP-Ang1. However the combination of both COMP and Ang-1 did not allow the investigators to dissect out the exact efficacy of Ang-1 in improving the impaired healing of wounds and to identify the underlying specific mechanism of action. In addition the study did not address the issue of a possible interplay between Ang-1 and VEGF.

Therefore the aim of our study was to investigate the mechanism(s) underlying the beneficial effects of Angiopoietin-1 in the diabetes-induced impairment of wound healing.

MATERIALS AND METHODS

rAAV vector preparation and characterization.

Two recombinant AAV vectors were obtained in this study, expressing the Lac-Z reporter gene (control gene) and the cDNA for mouse Angiopoietin-1 (Ang-1) under the control of the strong and constitutive cytomegalovirus (CMV) immediate early promoter. Both constructs were based on plasmid pFU-5, kindly provided by N. Muzyczka (University of Florida, Gainesville, Fla., USA) [16]. pAAV-LacZ was obtained by substituting the GFP open reading frame with the Lac-Z gene from plasmid pCH110 (Pharmacia, Uppsala, Sweden). The cDNA for Ang-1 was obtained by RT-PCR amplification of total RNA with appropriate primer pairs and again cloned to replace GFP in the pFU-5 vector digested with Bam HI and Eco RI. Infectious vector stocks were generated in 293 cells, cultured in 150-mm-diameter Petri dishes, by cotransfecting each plate with 15 µg of each vector plasmid, together with 45 µg of the packaging/helper plasmid, pDG (kindly provided by J.A. Kleinschmidt) expressing AAV and adenovirus helper functions [17]. Twelve hours after transfection, the medium was replaced by fresh medium and 3 days later the medium was collected and the cells harvested by scraping. After three freeze-thaw cycles in dry ice/ethanol bath and 37°C water bath, cell lysates were fractionated using ammonium sulphate precipitation. rAAV particles were then purified by CsCl gradient centrifugation in a SW41Ti rotor at 288,000×g for 36 h. Twelve to sixteen fractions of ten drops each were collected by inserting a G-21 needle below the rAAV band and their refractive index was determined. The six fractions with index closest to 1.3715 (corresponding to a density of 1.40 g/cm³) were dialyzed against phosphate buffered saline (PBS) at 4°C overnight and stored at -80°C. rAAV titres were determined by measuring the copy number of viral genomes in pooled, dialyzed gradient fractions. This was achieved by a competitive PCR procedure [18] using primers and competitors mapping in the CMV promoter region common to all vectors. The purified viral preparations used for this work had particle titres of about 1×10¹² viral genomes per ml. The infectious titre in this preparation is usually 100 to 1000 times less, depending on either the type of viral preparation and the target tissue. Each animals received the same dose of rAAV as stated in the experimental plan.

Animals

All procedures complied with the standards for care and use of animal subjects as stated in the Guide for the Care and Use of Laboratory animals (Institute of Laboratory Animal Resources, National Academy of Sciences, Bethesda, MD). Female genetically diabetic C57BL/KsJ *Lep^{db}* (hereinafter *db⁺/db⁺*) mice and their normoglycaemic littermates C57BL (hereinafter *db^{+/+}m*) were produced by the Jackson Laboratories and obtained from Charles River Laboratories (Pordenone, Italy). Animals were 14 weeks old at the start of the experiments. Diabetic mice were obese and severely insulin resistant as evidenced by hyperglycemia (plasma glucose 560 +/- 70 vs. 143 +/- 8 mg/dl in *db^{+/+}m*, $p < 0.05$) and hyperinsulinemia (plasma insulin 14.2 +/- 0.48 vs. 1.43 +/- 0.05 ng/ml in *db^{+/+}m*, $p < 0.05$) compared to nondiabetic animals. Diabetic mice weighed 30–32 g, whereas nondiabetic littermates weighed 22–24 g. The animals were housed one per cage maintained under controlled environmental conditions (12-h light/dark cycle, temperature ~23°C), and provided with standard laboratory food and water ad libitum.

Experimental protocol

After general anesthesia with thiopental sodium (80 mg/kg/i.p.), the hair on the back was shaved and the skin washed with povidone-iodine solution and wiped with sterile water. Two full-thickness longitudinal incisions (4 cm) were made on the dorsum of the mice, and the wound edges were closed with 4-0 silk surgical suture placed at 1-cm intervals. 10 animals for each group were killed after 7 and 14 days, respectively, and the wounds were divided into three segments (0.8 cm wide and 1.2 cm long). The caudal and cranial strip were used for molecular analysis and wound breaking strength, whereas the central one was used for histological and immunohistochemical evaluations. The animals were randomized to receive a single dose of either rAAV encoding for Ang-1 (~100µl; 1×10^{11} viral particles) or rAAV encoding for Lac-Z (~100µl; 1×10^{11} viral particles). Both rAAV were administered in the wound edges immediately after incision through 8 intra-dermal injections with a total volume of ~100µl, thus infecting the 100% of wound area.

Real Time PCR for ANG-1 and VEGF mRNA

Total RNA was extracted from skin by using a commercial kit (Trizol Reagent, Invitrogen, USA) according to manufacturer's instruction and spectrophotometrically quantified (Biophotometer, Eppendorf, USA). Total RNA was then treated with DNaseI

to digest residual DNA contamination, subsequently 5µg of total RNA was reverse transcribed using High capacity cDNA Archive Kit (Applied Biosystems, USA) and random primers according to manufacture's instruction. 10 ng of total cDNA was used to quantitate the amount of Ang-1 and VEGF-cDNA by Real Time Polymerase Chain Reaction method (Real-Time PCR), as well as β-actin cDNA as endogenous control. Both reactions were carried out in the same microwell (biplex) with Taq Man Universal PCR master mix and Assays on Demand ready to use primers and probes with different reporter dye (Applied Biosystems).

The progression of PCRs was monitored by 7300 Real Time-PCR System (Applied Biosystems), and the relative quantitation was determined by standard curve method for both target and endogenous reference. After normalization, the median of Ang-1 and VEGF levels in normal skin from control mice was considered as calibrator (1x sample) and the results were expressed as an n-fold difference relative to normal controls (relative expression levels).

The skin from diabetic and non diabetic mice not subjected to rAAV injection were also tested.

Determination of Angiopoietin-1, VEGFR1, VEGFR2 and eNOS by Western blot analysis

Briefly, skin samples were homogenized in 1 ml lysis buffer (20mM Hepes pH7.6, 50mM β-glycerophosphate, 1.0 mM DTT, 2.0 mM EGTA, 1% Triton, 10% glycerol) added with proteases and phosphatases inhibitors (2mM phenyl methyl sulfonyl fluoride, 1mg/ml aprotinin, 2mg/ml pepstatin A, 5mg/ml leupeptin and 100mM Na₃VO₄) with a Ultra Turrax (IKA, Staufen, Germany) homogenizer. The homogenate was subjected to centrifugation at 15.000 g for 15 min at 4°C. The supernatant was collected and used for protein determination using the Bio-Rad protein assay kit (Bio-Rad, Richmond, CA, USA).

Protein samples (30 µg) were denatured in Laemmli sample buffer (Bio-Rad) with 5% β-mercaptoethanol and separated by electrophoresis on an SDS (12%) polyacrylamide gel. The separated proteins were transferred on to a nitrocellulose membrane by using the transfer buffer (39 mM glycine, 48 mM Tris pH 8.3, 20% methanol) at 200 mA for 1 h. The membranes were stained with Ponceau' S (0.005% in 1% acetic acid) to confirm equal amounts of protein and were blocked with 5% non fat dry milk in TBS-

0.1% Tween for 1h at room temperature, washed three times for 10 min each in TBS-0.1% Tween, and incubated with a primary antibody for Ang-1, VEGFR1, VEGFR2 and for the constitutive and phosphorylated form of eNOS (Ser1177) (Chemicon, Temecula, CA, USA and Cell Signaling, Danvers, MA, USA) in TBS-0.1% Tween overnight at 4 °C. After being washed three times for 10 min each in TBS-0.1% Tween, the membranes were incubated with a specific secondary antibody peroxidase-conjugated (Pierce, UK) for 1 h at room temperature. After washing, the membranes were analyzed by the enhanced chemiluminescence system according to the manufacture's protocol (Amersham, NJ, USA). The protein signal was quantified by scanning densitometry using a bio-image analysis system (Bio-Profil, Celbio, Milan, Italy). The results from each experimental group were expressed as relative integrated intensity compared with normal skin measured with the same batch. Equal loading of protein was assessed on stripped blots by immunodetection of β -actin with a rabbit monoclonal antibody (Cell Signaling) diluted 1:500 and peroxidase-conjugated goat anti-rabbit immunoglobulin G (Pierce, UK) diluted 1:15000. All antibodies are purified by protein A and peptide affinity chromatography.

Determination of VEGF in wounds

The amount of VEGF in wounds was determined by an enzyme-linked immunoassorbent assay (ELISA). Briefly tissues were homogenized in 1.0 ml of 1 x phosphate-buffered saline containing complete protease inhibitor cocktail (Boehring Mannheim Indianapolis, IN). Homogenates were centrifuged to remove debris and were filtered through a 1.2- μ m pore syringe filter. Analysis was performed with a commercially available VEGF-specific ELISA kit (R&D Systems). The amount of VEGF was expressed as picograms per wound.

Determination of NO₂⁻/NO₃⁻

Wound samples were frozen in liquid nitrogen until use. NO products, were determined in wound lysates using the Griess reaction. Skin wounds samples were homogenized in 2 x lysis buffer (1 x lysis buffer: 1% Triton x-100, 20 mM Tris/HCL, pH 8.0, 137 mM NaCl, 10% glycerol, 5 mM EDTA, 1 mM phenylmethylsulfonyl fluoride, 15 μ g/ml leupeptin). The tissue extract was cleared by centrifugation and the supernatant was diluted 1:1 with water. Lysate (1 ml) were cleared by a centrifugation step at 100.00 x g for 30 mins. Cleared wound lysates (200 μ l) were adjusted to 4° C and mixed with 20

μl sulfanilamide (dissolved in 1.2M HCL) and 20 μl N-naphtylethyldiamine dihydrochloride. After 5 min at room temperature, the absorbance was measured at 540 nm with a reference wave-length at 690 nm. Combined $\text{NO}_2^-/\text{NO}_3^-$ levels were determined by reducing NO_2^- to NO_3^- with nitrate reductase in the presence of reduced nicotinamide adenine dinucleotide phosphate. For this, 80 μl of samples were incubated with 10 μL of *Aspergillus* nitrate reductase (1 unit/ml, Sigma, St. Louis MO) and 10 μL of NDPH 1 mmol/L for 1 hr at 27°C before the addition of the Griess reagent. All samples and standards, were assayed in triplicate. Data were expressed as mean \pm SD of $\text{NO}_2^-/\text{NO}_3^-$.

Phenylmethylsulfonyl fluoride, leupeptin, and N-naphtylethyldiamine dihydrochloride, were obtained from Sigma Biochemicals (St. Louis, MO).

Histology

All tissue specimens were fixed in 10% neutral buffered formalin for at least 24h at room temperature. After fixation, perpendicular sections to the anterior-posterior axis of the wounds were dehydrated in graded ethanol, cleared in xylene, and embedded in paraffin. Five-micron-thick sections were mounted on glass slides, dewaxed, rehydrated with distilled water, and stained with hematoxylin and eosin or with Masson's trichrome according to routine procedures for light microscopy. For the amount of granulation tissue the areas proximal to the incision were evaluated by three blinded pathologists in the all section of each slide. As part of the histological evaluation, all slides were examined by a pathologist without knowledge of the previous treatment by means of an eyepiece grid under the microscope from x5 to x100 magnification. The following parameters were evaluated and scored: reepithelialization, dermal matrix deposition and regeneration, granulation tissue formation and remodelling and angiogenesis. The edges of the wound in each of the sections as well as normal control wounds were used as comparison for scoring.

Immunohistochemistry

Paraffin-embedded tissues were sectioned (5 μm), and antigen retrieval was performed using 0,05M sodium citrate buffer. Tissues were treated with primary antibody against PECAM-1 (Santa Cruz, USA), VEGFR-2 (Cell Signaling) and VEGFR-1 (Abcam, UK). Secondary antibody was provided by Pierce, and the location of the reaction was

visualized in brown with 3,3'-diaminobenzidine tetra-hydrochloride (Sigma) and nuclear fast red counter stain was used. Slides were then mounted with coverslips.

To assess angiogenic response, microvessel density (MVD) was estimated after PECAM-1 staining. Briefly, five areas per section were randomly selected in the dermis just proximal to the wound site and the positive endothelial cells were counted per high-power field (x40 magnification) by three pathologists blinded to the samples. To assess positive VEGFR-1 and VEGFR-2 staining five areas per section were randomly selected in the dermis and the positive endothelial cells were counted per high-power field (x40 magnification) by three pathologists blinded to the samples.

In each reaction a positive control of human angiosarcoma was used. For negative controls, the primary antibodies were replaced by citrate buffer (pH 6.0).

Breaking strength.

The maximum load (breaking strength) tolerated by wounds was measured blindly on coded samples using a calibrated tensometer (Instron Corp, Canton, Mass., USA) as described previously [19]. The ends of the skin strip were pulled at a constant speed (20 cm/min), and breaking strength was expressed as the mean maximum level of tensile strength (g/mm) before separation of wounds.

In vivo vascular permeability

In vivo vascular permeability was evaluated in an additional set of animals. Briefly, Female genetically diabetic C57BL/KsJ *Lep^{db}* (*db⁺/db⁺*) mice and their normoglycaemic littermates C57BL (*db^{+/+}m*) treated either with rAAV encoding for Ang-1 (~100µl; 1x10¹¹ viral particles) or rAAV encoding for Lac-Z (~100µl; 1x10¹¹ viral particles). On the day of trial (day 14) the mice were intradermally injected with 5 µg of compound 48/80 (Sigma, St. Louis MO) dissolved in 50 µl of physiological saline into the wound edges. Compound 48/80 administration is followed by increased leukocyte rolling, increased leukocyte adhesion and increased vascular permeability in postcapillary venules. Immediately after an intravenous injection of a 0.5% Evans blue solution (5 ml/kg/mouse). Animals were sacrificed 30 minutes after the compound 48/80 injection and the skin of the reaction locus was removed for a quantitative determination of the extravasated dye. Evans blue was extracted from each piece of dissected skin with 1 ml of 6M KOH at 45°C for 6 h. This extract was neutralized by 1 ml of 6M HCL, and then 2 ml of acetone was added. The extract was clarified by filtration, its absorbance at 595

nm was measured, and the extracted Evans blue content was then calculated from its calibration curve.

Statistical Analysis

All data are expressed as the mean plus or minus the standard deviation (mean \pm SD). Before analysis all end points were tested for normality by using the Kolmogorov-Smirnov test. The test suggested that data were normally distributed therefore they were analysed using a two-way ANOVA.

In all cases, a probability error of less than 0.05 was selected as criterion for statistical significance.

RESULTS

Efficacy of Ang-1 gene transfer in wounds.

Angiotensin-1 is normally expressed in the skin during adult life and is not affected by diabetes. The efficacy of rAAV mediated gene transfer was assessed by either Real-Time PCR and western blot analysis at day 7 and 14 after wounding. The unwounded skin from diabetic and non diabetic mice not subjected to rAAV injection, showed levels of Ang-1 mRNA comparable to those obtained from rAAV-Lac-Z injected animals (diabetic= 5.5 ± 1 n-fold vs β -actin; non diabetic= 5.1 ± 0.8 n-fold vs β -actin). At day 7 after injury the expression of Ang-1 mRNA was slightly increased in the wounds of diabetic animals administered with (5.7 ± 0.9 n-fold vs β -actin); while Ang-1 gene transfer significantly augmented Ang-1 mRNA expression at each time point (day 7= 11.4 ± 1.7 n-fold vs β -actin; $p < 0.001$ vs rAAV for Lac-Z), (Figure 1). Similar results were obtained in non diabetic animals (Figure 1).

The enhanced mRNA expression for the angiogenic factor resulted in an increased protein expression 7 and 14 days after wounding, as confirmed by western blot analysis, in either normoglycaemic (11.5 ± 1.1 relative units of integrated intensity; $p < 0.001$ vs rAAV-Lac-Z at day 7) and diabetic mice (12.4 ± 1 relative units of integrated intensity; $p < 0.001$ vs rAAV Lac-Z at day 7) administered with rAAV-Ang-1 at each time point (Figure 2).

Expression of eNOS in wounds

Uninjured skin had a very low content of p-eNOS (1.1 ± 0.9 and 0.5 ± 0.08 integrated intensity, in normoglycaemic and diabetic animals respectively). Wounding caused at day 7 an enhanced expression of p-eNOS in both strain of animals (normoglycaemic animals = 7.1 ± 1.6 integrated intensity; diabetic animals = 4 ± 1.7 integrated intensity; Figure 3A). In wounds treated with rAAV-Ang-1 we found an higher increase in p-eNOS in both normoglycaemic (13.1 ± 1.5 integrated intensity) and diabetic animals (10.2 ± 1.4 integrated intensity; Figure 3A).

NO products in wounds

We determined the concentration of $\text{NO}_2^-/\text{NO}_3^-$ in wound lysates from rAAV-Lac-Z or with rAAV-Ang-1 injected normoglycaemic and diabetic mice. Wounding caused at day 7 a marked increase in $\text{NO}_2^-/\text{NO}_3^-$ content compared to control uninjured skin (normoglycaemic animals= 3.3 ± 0.6 nmol g tissue; diabetic animals= 1.1 ± 0.08 nmol/g

tissue). We observed a stronger increase in wound NO products in mice subjected to the Ang-1 rAAV-mediated gene transfer (Figure 3B).

Histological assessment.

Delivery of Ang-1 in the wound edge produced a significant improvement in the healing process as shown by the hematoxylin-eosin staining and by Masson's trichrome staining for the assessment of epidermal regeneration and the thickness of granulation tissue (Figure 4 and 5). Complete skin normalization in untreated mice occurred at day 22 ± 1 after wounding in non-diabetics and at day 35 ± 2 in diabetics. No side effect, nor signs of inflammation were noted in either diabetic and normoglycaemic animals injected with the viral vectors. Diabetic animals usually have a thicker epithelial layer than normal mice, in addition the different layers are less differentiated and adipose infiltrates are present in dermis, impairing the normal elasticity of the skin that in consequence is more prone to a delayed healing.

At day 14 wounds of diabetic animals administered with rAAV-Lac-Z showed a still incomplete reepithelialization, the presence of a crust, a very low organized granulation tissue and a marked adipose substitution in the dermis. By contrast, at the same time point rAAV-Ang-1-treated diabetic wounds demonstrated a complete reepithelialization, well-organized dermal layers, well-formed granulation tissue, reduced adipose substitution and mature collagen bundles (Figure 4 and 5).

Non diabetic animals injected with rAAV-Lac-Z showed almost complete reepithelialization at day 14, the administration of rAAV-Ang-1 resulted in an improved reepithelialization process as demonstrated by the presence of hair follicles in the dermis (Figure 4 and 5).

Evaluation of new blood vessel formation

PECAM-1 immunostaining was investigated 14 days after surgical procedures to confirm neo-vessel formation (Figure 6). In fact, it represents a highly specific marker for endothelial cells. As reported in the figure the positive staining in the granulation tissue of diabetic rAAV-Ang-1 injected animals was mostly expressed by small vessels and capillaries, while in those receiving rAAV-Lac-Z reactivity was found only in pre-existing vessels, demonstrating an augmented angiogenesis mediated by Ang-1 administration.

Using the images obtained by PECAM-1 staining the tissue samples from each group were assessed for microvessel density as reported in figure 6.

Breaking strength.

Angiopoietin-1 gene transfer improved the tensile strength of the injured tissue as shown in Figure 7 which summarizes the wound breaking strength values obtained for each group at day 14. The breaking strength of incisional diabetic wounds of animals treated with recombinant AAV vector encoding Ang-1 was higher than that of diabetic wounds obtained from mice given with rAAV-LacZ. Similar results were observed in wounds obtained from non-diabetic animals (Figure 7).

VEGF mRNA and protein expression

To understand the basis of the angiogenic process we investigated the expression of VEGF in wounds by Real Time PCR at day 7 and 14 after injury. In fact diabetic animals show a distorted VEGF pattern which is responsible of an inadequate angiogenetic process. In the wounds of diabetic mice administered with rAAV-Lac-Z, VEGF mRNA was markedly lower than in normoglycaemic animals at each time point ($p < 0.001$ vs normoglycaemic animals). Treatment with rAAV-Ang-1 did not modified the disturbed VEGF mRNA expression in diabetic mice at day 7 and 14 (p not significant vs rAAV-Lac-Z), (Figure 8A).

Non-diabetic rAAV-Lac-Z treated mice showed a normally marked induction of VEGF mRNA at day 7 that declined to normal values following 14 day after injury and this expression was not affected by Ang-1 gene transfer (p not significant vs rAAV-Lac-Z) suggesting that Angiopoietin-1 is not able to induce VEGF expression (Figure 8A).

To confirm this result, we also investigated VEGF protein by ELISA. Overlapping data were obtained (Figure 8B). Administration of rAAV-Ang-1 did not modified the disturbed VEGF protein production in diabetic mice at day 7 and 14 (p not significant vs rAAV-Lac-Z), (Figure 8B). In addition rAAV-Lac-Z treated mice showed a normally marked VEGF protein expression at day 7 that declined to normal values following 14 day after injury and this expression was not affected by Ang-1 gene transfer (p not significant vs rAAV-Lac-Z) confirming that Angiopoietin-1 is not able to induce VEGF expression (Figure 8B).

Assessment of VEGFR-2 immunostaining and protein expression.

At day 7 we performed the immunostaining for VEGFR-2, a marker that identifies endothelial precursor cells [10, 20]; these cells are not only circulating and bone marrow-derived, but they are also present in the subcutaneous adipose tissue. Ang-1 rAAV-mediated gene transfer augmented VEGFR-2 expression in endothelial cells in diabetic animals (Figure 9), thus contributing to the healing process. Similar results were obtained in normoglycaemic animals (results not shown). In contrast a very slight staining for the VEGFR-1 receptor, that is mostly expressed by mature endothelial cells, was observed in both strains of mice administered with rAAV-Ang-1, further suggesting that VEGF is not involved in Angiopoietin-1 driven angiogenesis. However both Angiopoietin-1 and VEGF are able to recruit endothelial precursors [10, 20].

To confirm this result we quantified VEGFR protein expression by Western Blot analysis in skin wounds. A low expression of VEGFR-1 protein was present in normoglycaemic and diabetic animals injected with rAAV-Ang-1 (Figure 10A). By contrast Ang-1 rAAV-mediated gene transfer enhanced VEGFR-2 protein (Figure 10A).

In vivo vascular permeability

At day 14 we evaluated in vivo vascular permeability by administering compound 48/80 which causes Evans blue leakage. As shown in Figure 10B and intradermal stimulation of 5 µg of compound 48/80 caused a significantly leakage of Evans Blue that has been intravenously injected before compound 48/80. No significant difference were observed among the several groups treated either with rAAV-Lac-Z or rAAV-Ang-1.

DISCUSSION

Blood vessels form through two distinct processes, vasculogenesis and angiogenesis [21]. In vasculogenesis, endothelial cells differentiate *de novo* from mesodermal precursors, whereas in angiogenesis new vessels are generated from pre-existing ones. Angiogenesis and neovascularization can be unwanted processes in certain diseases, including cancer and diabetic retinopathy. However, formation of the new blood vessels can also help alleviate some states, as in the formation of collateral circulation in ischemic myocardium, limbs as well as during the healing of wounds.

VEGF and Ang-1 have strong effect on angiogenesis and vasculogenesis respectively. VEGF specific activities include endothelial cell survival, proliferation, migration and tube formation; while Ang-1 has no proliferative effect, but it is a strong inducer of vasculogenesis recruiting and differentiating mesodermal resident precursors as well as bone marrow-derived EPCs. These cells present the surface marker VEGFR-2 (or *flk-1*) specific for the committed as well as for the young endothelial cells and, driven by growth factors, migrate from the lateral plate mesoderm toward the dorsal aorta to the site of neovascularization [20-23].

In our experiment the rAAV mediated gene transfer of Ang-1 improved the altered healing process, enhanced the impaired angiogenesis and increased wound breaking strength in diabetic animals. However Ang-1 gene transfer did not modify the disturbed pattern of VEGF expression. In contrast Ang-1 stimulated the expression of VEGFR-2 in new vessels close to the wound site in genetically diabetic mice.

In diabetes the need of neovascularization arises from the inadequate VEGF production and release in wounds: thus, the classic angiogenetic process is extremely delayed and poor and, as a consequence, therapeutically valuable approaches have been addressed to the aim of stimulating the expression of the impaired angiopoietic factor [24]. However our results clearly suggest that active angiogenesis may also occur in diabetes without the involvement and intervention of VEGF. Under these specific circumstances, vasculogenesis may represent an alternative pathway to induce new blood vessel formation. More specifically our data strongly suggest that Ang-1 causes, at least in diabetes, angiogenesis in a VEGF independent manner and likely through the endothelial progenitor cells. The enhanced PECAM-1 staining in endothelial cell at the wound site confirms an active angiogenesis. It could be hypothesized that the slightly

positive staining for VEGFR-1 is reliant to the low but still present VEGF protein presence in the skin of diabetic animals after the surgical injury. On the other hand the marked staining for VEGFR-2 after Ang-1 administration could be related to the presence of endothelial precursors, that usually present this marker [2, 10].

To date, it is well established that NO substantially regulates wound matrix deposition [25], as inhibition of wound NO synthesis was paralleled by decreased wound collagen accumulation and wound breaking strength. Interestingly we found active eNOS protein to be low expressed at the wound site in diabetes impaired healing in *db/db* mice. This observation clearly suggests that in the diabetic wound healing process there is also a defect in nitric oxide pathway that might also contribute to impair the healing process. Ang-1 gene transfer succeeded in reverting the impairment in nitric oxide: in fact rAAV-Ang-1 increased both eNOS expression and NO production. Therefore the activation of this NO pathway might represent an additional Ang-1 mechanism of action, acting in concert angiopoietin-1 and eNOS are able to sustain an effective improvement in new vessels formation.

In conclusion the present experimental observations are extremely relevant in the management of diabetic patients which display a delayed wound healing: in fact our results provide strong evidences that Ang-1 gene transfer improves the delayed wound repair in diabetes by stimulation of angiogenesis, apparently without VEGF involvement, that could be more detrimental than useful as it happens during diabetic retinopathy. Furthermore unpublished observations from our laboratory suggest that VEGF gene transfer does not affect Ang-1 expression and the combined delivery of VEGF and angiopoietin-1 does not cause a greater effect than the delivery of one of the two angiogenic factors. Whether this finding might have important clinical correlates, remains at the moment a still-open issue that deserves further pre-clinical and clinical investigations.

REFERENCES

- 1) Conway, E.M., Collen, D., and Carmeliet, P. (2001) Molecular mechanisms of blood vessel growth. *Cardiovasc. Res.* 49, 507-521.
- 2) Ferrara, N., Gerber, H.P., and LeCouter, J. (2003) The biology of VEGF and its receptors. *Nat. Med.* 9, 669-676.
- 3) Tammela, T., Enholm, B., Alitalo, K., and Paavonen, K. (2005) The biology of vascular endothelial growth factors. *Cardiovasc. Res.* 65, 550-563.
- 4) Goodson, W.H., and Hunt, T.K. (1977) Studies of wound healing in experimental diabetes. *J. Surg. Res.* 22, 221-227.
- 5) Bohlen, H.G., and Niggli, B.A. (1979) Adult microvascular disturbances as a result of juvenile-onset diabetes in *db/db* mice. *Blood. Vessels.* 16, 269-276.
- 6) Altavilla, D., Saitta, A., Cucinotta, D., et al. (2001) Inhibition of lipid peroxidation restores impaired vascular endothelial growth factor expression and stimulates wound healing and angiogenesis in the genetically diabetic mouse. *Diabetes.* 50, 667-674.
- 7) Galeano, M., Deodato, B., Altavilla, D., et al. (2003) Adeno-associated viral vector-mediated human vascular endothelial growth factor gene transfer stimulates angiogenesis and wound healing in the genetically diabetic mouse. *Diabetologia.* 46, 546-555.
- 8) Peichev, M., Naiyer, A.J., Pereira, D., et al. (2000) Expression of VEGFR-2 and AC133 by circulating human CD34⁺ cells identifies a population of functional endothelial precursors. *Blood.* 95, 952-958.
- 9) Asahara, T., Murohara, T., Sullivan, A., et al. (1997) Isolation of putative progenitor endothelial cells for angiogenesis. *Science.* 275, 964-967.
- 10) Urbich, C., and Dimmeler, S. (2004) Endothelial progenitor cells functional characterization. *Trends. Cardiovasc. Med.* 14, 318-22. Review.
- 11) Wetzler, C., Kampfer, H., Stallmeyer, B., Pfeilschifter, J., and Frank, S. (2000) Large and sustained induction of chemokines during impaired wound healing in the genetically diabetic mouse: prolonged persistence of neutrophils and macrophages during the late phase of repair. *J. Invest. Dermatol.* 115, 245-253.

- 12) Holash, J., Maisonpierre, P.C., Compton, D., et al. (1999) Vessel cooption, regression, and growth in tumors mediated by angiopoietins and VEGF. *Science*. 284, 1994-1998.
- 13) Babaei, S., Teichert-Kuliszewska, K., Zhang, Q., Jones, N., Dumont, D.J., and Stewart, D.J. (2003) Angiogenic actions of angiopoietin-1 require endothelium-derived nitric oxide. *Am. J. Pathol.* 162, 1927-1936.
- 14) Stadelmann, W.K., Digenis, A.G., and Tobin, G.R. (1998) Impediments to wound healing. *Am. J. Surg.* 176, 39S-47S.
- 15) Cho, C.H., Sung, H.K., Kim, K.T., et al. (2006) COMP-angiopoietin-1 promotes wound healing through enhanced angiogenesis, lymphangiogenesis, and blood flow in a diabetic mouse model. *Proc. Natl. Acad. Sci. U S A.* 103, 4946-4951.
- 16) Zolotukhin, S., Putter, M., Hauswirth, W.W., Guy, J. and Muzyczka, N. (1996) A "humanized" green fluorescent protein cDNA adapted for high-level expression in mammalian cells. *J. Virol.* 70, 4646-4654.
- 17) Grimm, D., Kern, A., Rittner, K. and Kleinschmidt, J.A. (1998) Novel tools for production and purification of recombinant adenoassociated virus vectors. *Hum. Gene. Ther.* 9, 2745-2760.
- 18) Diviacco, S., Norio, P., Zentilin, L. et al. (1992) A novel procedure for quantitative polymerase chain reaction by coamplification of competitive templates. *Gene.* 122, 313-320.
- 19) Pierce, G.F., Mustoe, T.A., Senior, R.M., Reed, J., Griffin, G.L., Thomason, A., Deuel, T.F. (1988) In vivo incisional wound healing augmented by platelet-derived growth factor and recombinant c-cis gene homodimeric proteins. *J. Exp. Med.* 167, 974-987.
- 20) Asahara, T., Masuda, H. and Takahashi, T. (1999) Bone marrow origin of endothelial progenitor cells responsible for postnatal vasculogenesis in physiological and pathological neovascularization. *Circ. Res.* 85, 221-228.
- 21) Patan, S. (2004) Vasculogenesis and angiogenesis. *Cancer. Treat. Res.* 117, 3-32.
- 22) Visconti, R.P., Richardson, C.D. and Sato, T.N. (2002) Orchestration of angiogenesis and arteriovenous contribution by angiopoietins and vascular endothelial growth factor (VEGF). *PNAS.* 99, 8219-8224.

- 23) Shim, W.S., Li, W., Zhang, L. et al. (2006) Angiotensin-1 promotes functional neovascularization that relieves ischemia by improving regional reperfusion in a swine chronic myocardial ischemia model. *J. Biomed. Sci.* 13, 579-591.
- 24) Pandya, N.M., Dhalla, N.S., Santani, D.D. (2006) Angiogenesis-a new target for future therapy. *Vascul. Pharmacol.* 44, 265-274. Review.
- 25) Schaffer, M.R., Tantry, U., Efron, P.A., et al. (1997) Diabetes-impaired healing and reduced wound nitric oxide synthesis: a possible pathophysiologic correlation. *Surgery.* 121, 513–519.

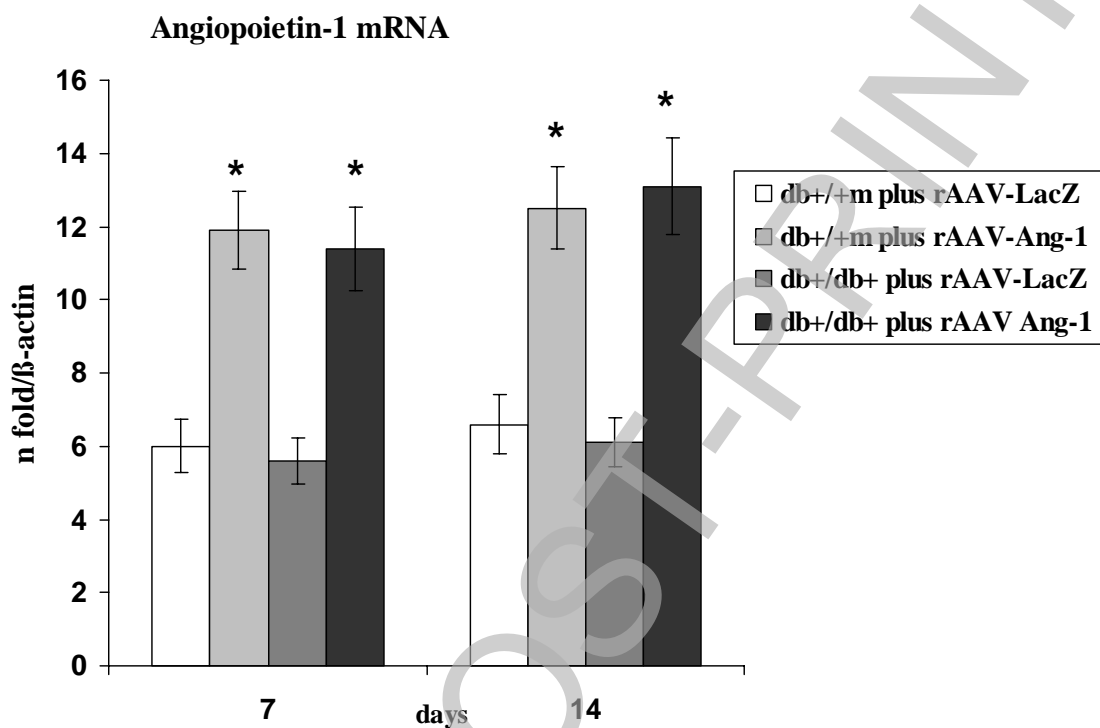


Figure 1

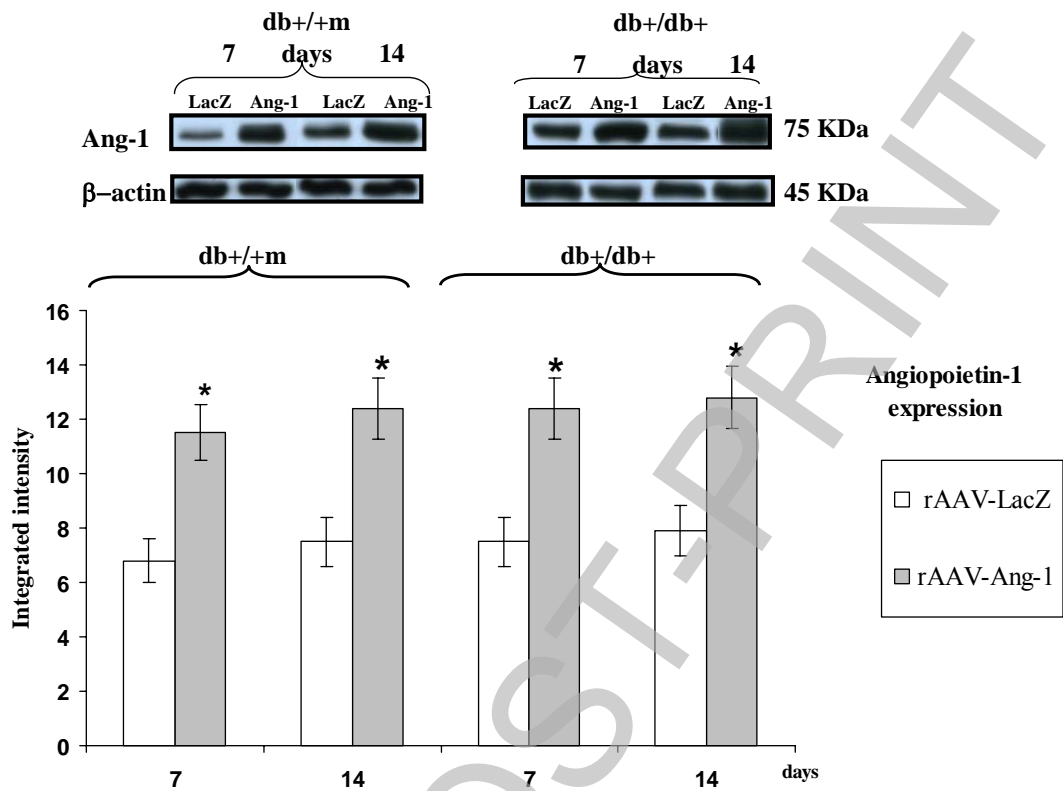


Figure 2

THIS IS NOT THE FINAL VERSION - see doi:10.1042/CS20070250

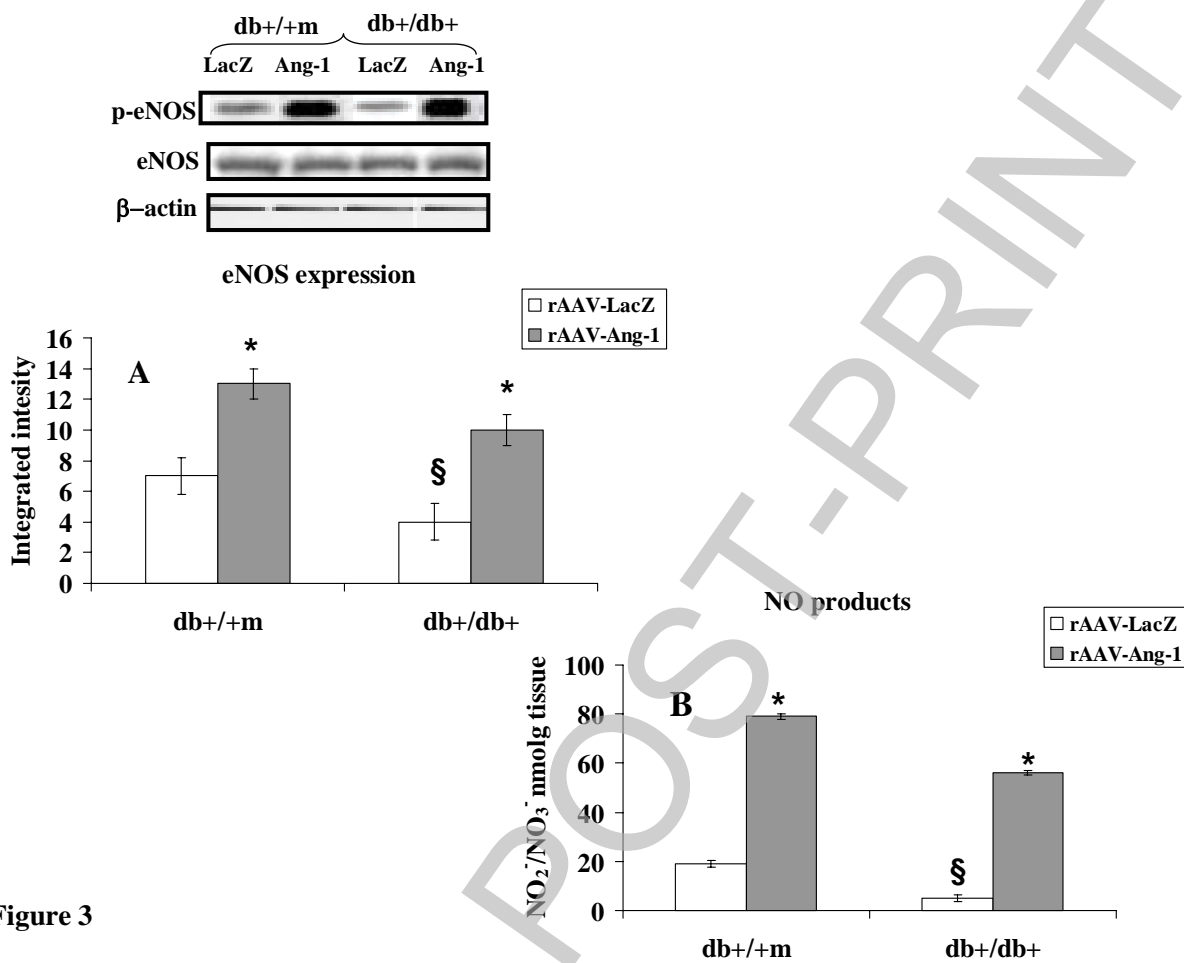


Figure 3

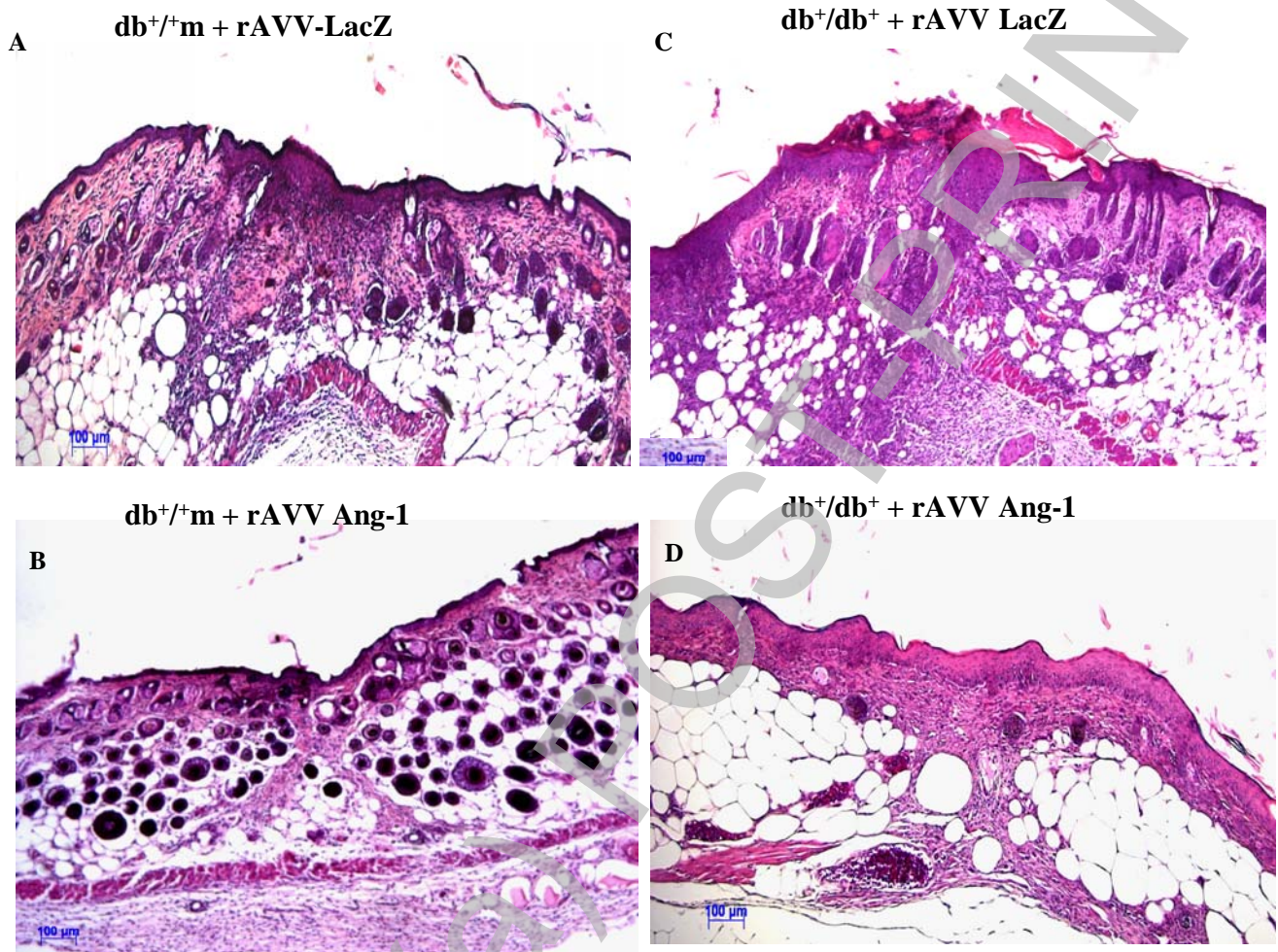


Figure 4

THIS IS NOT THE FINAL VERSION - see doi:10.1042/CS20070250

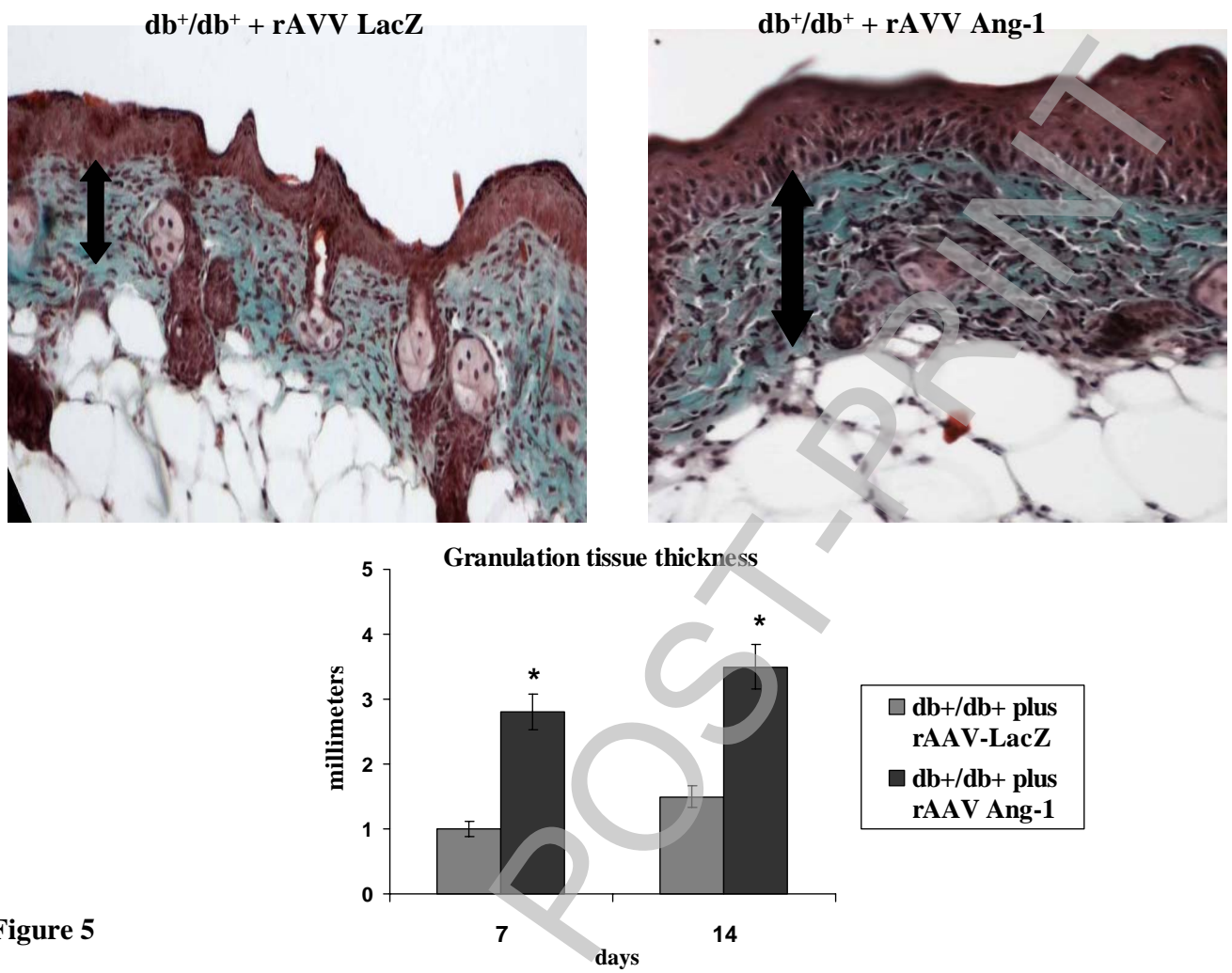


Figure 5

Stage 2(a)

THIS IS NOT THE FINAL VERSION - see doi:10.1042/CS20070250

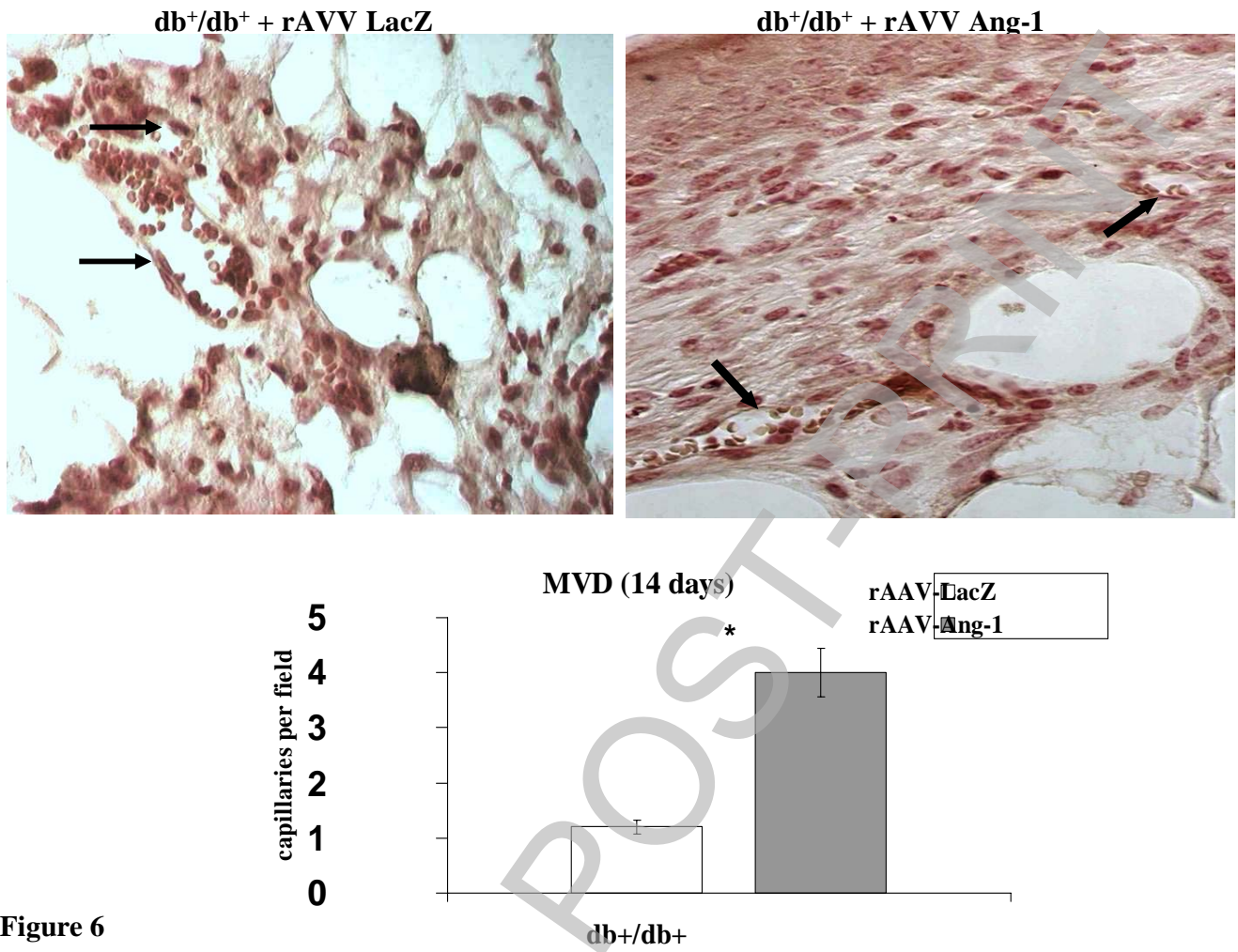


Figure 6

Stage 2(a)

THIS IS NOT THE FINAL VERSION - see doi:10.1042/CS20070250

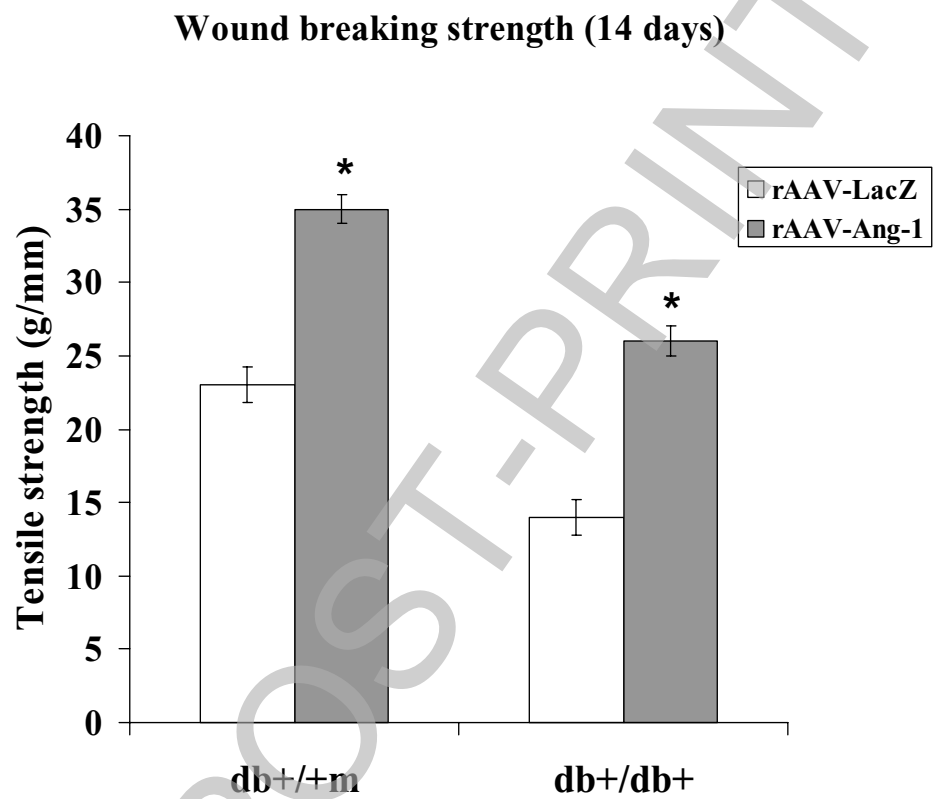


Figure 7

Stage 2(a) POST-PRINT

THIS IS NOT THE FINAL VERSION - see doi:10.1042/CS20070250

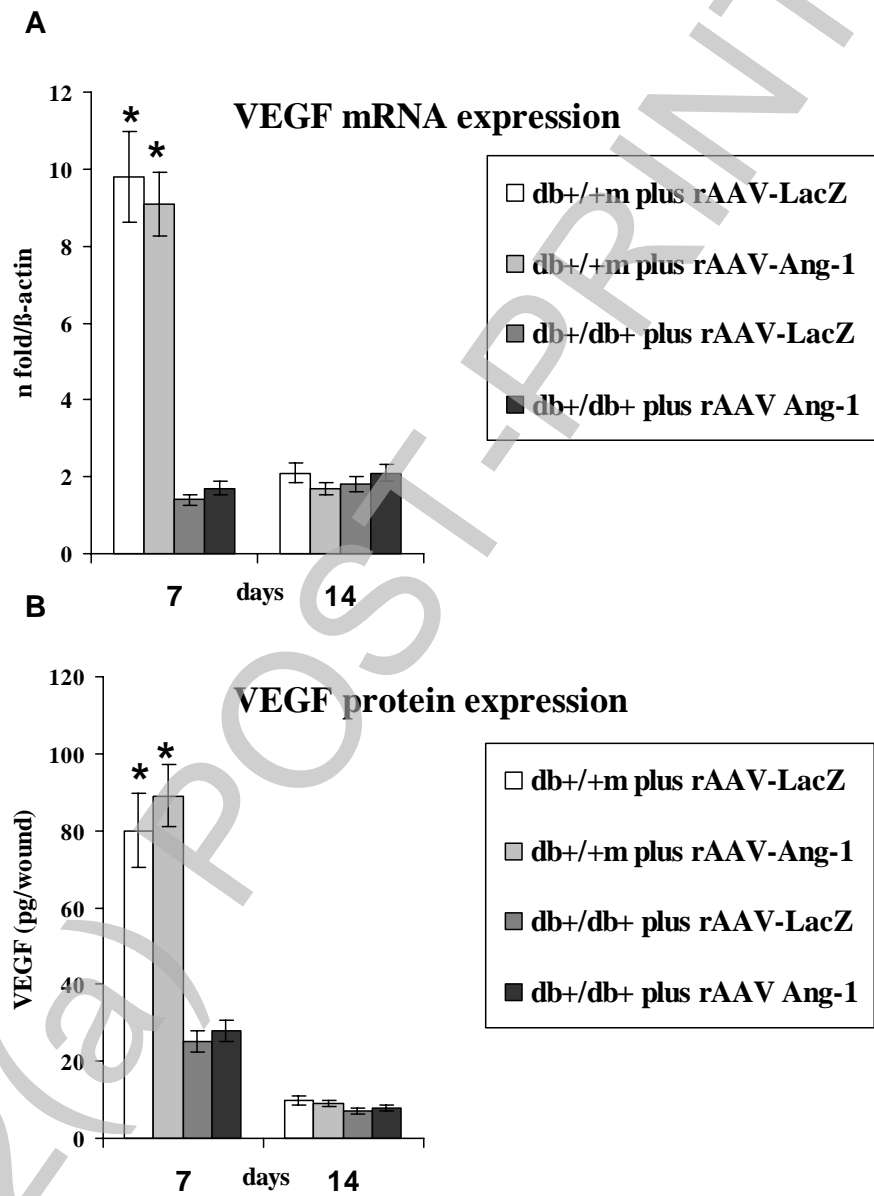


Figure 8

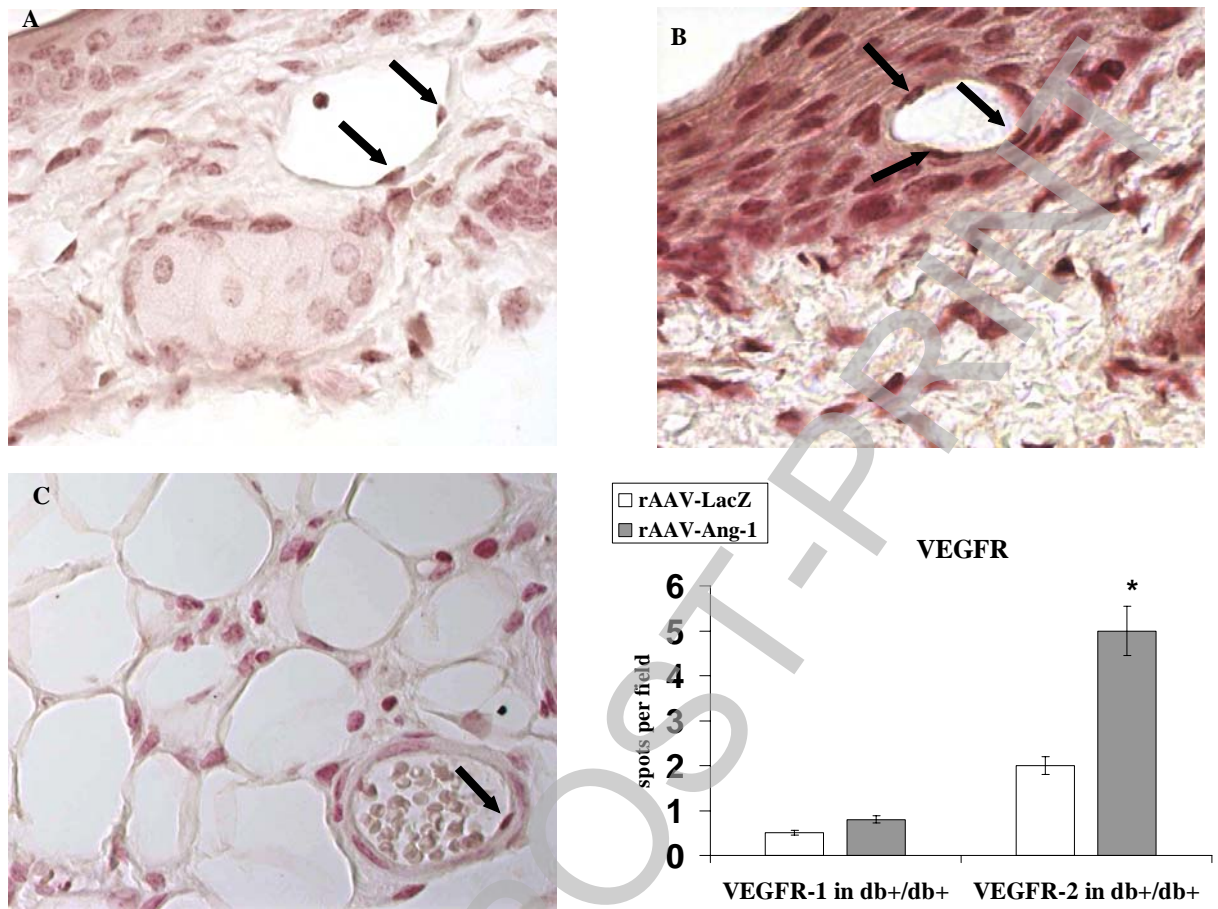


Figure 9

Stage 2(a) P

THIS IS NOT THE FINAL VERSION - see doi:10.1042/CS20070250

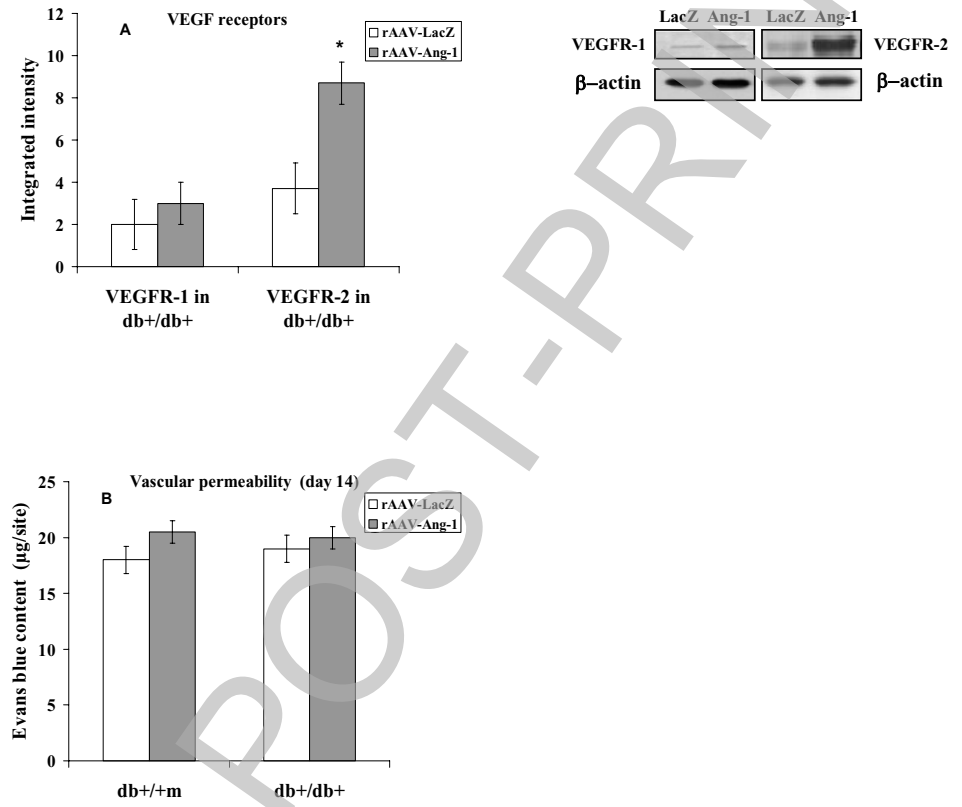


Figure 10

Stage 2(a)

FIGURE CAPTIONS

Figure 1.

Ang-1 mRNA levels evaluated by Real Time PCR in skin wound samples collected from either normoglycaemic ($db^{+/+}m$) and diabetic mice (db^{+}/db^{+}) given either rAAV-Lac-Z ($\sim 100\mu\text{l}$; 1×10^{11} viral particles) or rAAV-Ang-1 ($\sim 100\mu\text{l}$; 1×10^{11} viral particles). Each bar represents the mean \pm S.D. of seven experiments. * $p < 0.001$ vs rAAV-Lac-Z.

Figure 2.

Representative western blot analysis and a quantitative assessment of Ang-1 protein expression in skin wound specimens obtained from either normoglycaemic ($db^{+/+}m$) and diabetic mice (db^{+}/db^{+}) given rAAV-Lac-Z ($\sim 100\mu\text{l}$; 1×10^{11} viral particles) or rAAV-Ang-1 ($\sim 100\mu\text{l}$; 1×10^{11} viral particles). Each bar represents the mean \pm S.D. of seven experiments. * $p < 0.001$ vs rAAV-Lac-Z.

Figure 3

eNOS expression (constitutive and phosphorylated form) (A) and NO products (B) in skin wound samples collected from either normoglycaemic ($db^{+/+}m$) and diabetic mice (db^{+}/db^{+}) given either rAAV-Lac-Z ($\sim 100\mu\text{l}$; 1×10^{11} viral particles) or rAAV-Ang-1 ($\sim 100\mu\text{l}$; 1×10^{11} viral particles). Each bar represents the mean \pm S.D. of seven experiments. * $p < 0.001$ vs rAAV-Lac-Z; § $p < 0.05$ vs $db^{+/+}m$.

Figure 4.

Histological photomicrographs, haematoxylin-eosin, (original magnification $\times 10$.)

A: rAAV-LacZ-treated nondiabetic ($db^{+/+}m$) wound at day 14. Re-epithelialization is almost complete. Granulation tissue is well-formed without inflammatory infiltrates.

B: rAAV-Ang-1-treated nondiabetic ($db^{+/+}m$) wound at day 14. Complete re-epithelialization with presence of hair and restoration of normal architecture in dermis.

C: rAAV-LacZ-treated diabetic (db^{+}/db^{+}) wound at day 14. Thin and immature epithelial layer, with presence of crusting and poorly-formed granulation tissue.

D: rAAV-Ang-1-treated diabetic (db^+/db^+) wound at day 14. Re-epithelialization is almost complete with absence of spongiosis or crusting, well-organized granulation tissue and no evidence of inflammation, oedema or erythrorrhagies.

Figure 5.

Masson's trichrome staining of skin wound from either diabetic mice (db^+/db^+) administered with rAAV-Lac-Z (~100 μ l; 1×10^{11} viral particles) or rAAV-Ang-1 (~100 μ l; 1×10^{11} viral particles) at day 14 and quantification of collagen bundles.

Figure 6.

Representative immunohistochemical PECAM-1 staining of skin wounds samples from diabetic mice (db^+/db^+) given with rAAV-Lac-Z (~100 μ l; 1×10^{11} viral particles) or rAAV-Ang-1 (~100 μ l; 1×10^{11} viral particles) at day 14, (original magnification x40) and comparison of semiquantitative assessment of microvascular density (MVD) between each group. Each bar represents the mean \pm S.D. of seven experiments. * $p < 0.05$ vs rAAV-Lac-Z.

Figure 7.

Tensile strength of wounds obtained at day 14 from non diabetic ($db^{+/+}m$) and diabetic mice (db^+/db^+) administered with either rAAV-Lac-Z (~100 μ l; 1×10^{11} viral particles) or rAAV-Ang-1 (~100 μ l; 1×10^{11} viral particles). Each bar represents the mean \pm S.D. of seven experiments. * $p < 0.001$ vs rAAV-Lac-Z.

Figure 8.

VEGF mRNA levels evaluated by Real Time PCR (A) and VEGF protein studied by ELISA (B) in skin wound samples collected from either normoglycaemic ($db^{+/+}m$) and diabetic mice (db^+/db^+) given either rAAV-Lac-Z (~100 μ l; 1×10^{11} viral particles) or rAAV-Ang-1 (~100 μ l; 1×10^{11} viral particles). Each bar represents the mean \pm S.D. of seven experiments. * $p < 0.001$ vs rAAV-Lac-Z and diabetic animals.

Figure 9.

A and B: Representative immunohistochemical VEGFR-2 staining of skin wound samples from diabetic mice (db^+/db^+) given with rAAV-Lac-Z (~100 μ l; 1×10^{11} viral particles) or rAAV-Ang-1 (~100 μ l; 1×10^{11} viral particles) at day 7. (Original magnification x40).

C: Representative immunohistochemical VEGFR-1 staining of skin wound samples from diabetic mice (db^+/db^+) given with rAAV-Ang-1 ($\sim 100\mu\text{l}$; 1×10^{11} viral particles) at day 7. (Original magnification x40).

The graph represents the mean \pm S.D. of positive endothelial cells per field. * $p < 0.01$ vs rAAV-Lac-Z.

Figure 10.

- A.** VEGF receptors expression in skin wounds samples from diabetic mice (db^+/db^+) given with rAAV-Lac-Z ($\sim 100\mu\text{l}$; 1×10^{11} viral particles) or rAAV-Ang-1 ($\sim 100\mu\text{l}$; 1×10^{11} viral particles) at day 7. Each bar represents the mean \pm S.D. of seven experiments. * $p < 0.05$ vs rAAV-Lac-Z.
- B.** In vivo vascular permeability of normoglycaemic ($db^{+/+m}$) and diabetic mice (db^+/db^+) given either rAAV-Lac-Z ($\sim 100\mu\text{l}$; 1×10^{11} viral particles) or rAAV-Ang-1 ($\sim 100\mu\text{l}$; 1×10^{11} viral particles). Each bar represents the mean \pm S.D. of seven experiments. * $p < 0.001$ vs rAAV-Lac-Z and diabetic animals.